Meteoritics & Planetary Science 36, 947–961 (2001)
Available online at http://www.uark.edu/meteor

Noble gases in enstatite chondrites I: Exposure ages, pairing, and weathering effects

ANDREA PATZER†* AND LUDOLF SCHULTZ

Max-Planck-Institut für Chemie, D-55020 Mainz, Germany
†Present address: Lunar and Planetary Laboratory, University of Arizona, Tucson, Arizona 85721, USA
*Correspondence author's email address: apatzer@lpl.arizona.edu

(Received 2001 January 2; accepted in revised form 2001 April 6)

Abstract–Cosmic-ray exposure ages calculated from cosmogenic noble gas nuclides are reported for 57 enstatite (E) chondrites, 43 of them were measured for the first time. With a total of 62 individual E chondrites (literature and this data, corrected for pairing) the observed spectrum of ages ranges between 0.07 and 66 Ma. Three clusters seem to develop at about 3.5, 8, and 25 Ma, respectively. Since the uncertainty of ages is estimated to be ~20% (in contrast to 10 to 15% for ordinary chondrites) and the number of examined samples is still comparatively small, these peaks have to be confirmed by more measurements. Regarding the two subgroups, EH and EL chondrites, no systematic trend is apparent in the distribution of cosmic-ray exposure ages.

Several E chondrites yield significantly lower ^{38}Ar ages compared to those calculated from cosmogenic ^{3}He and ^{21}Ne. For these E chondrites, we suggest a reduction of cosmogenic ^{38}Ar as a result of weathering. In order to prove the possible influence of terrestrial alteration on the cosmogenic noble gas record of E-chondritic material, we simulated terrestrial weathering in an experiment of 12 weeks duration. The treatment showed that a significant amount of cosmogenic ^{38}Ar is lost on Earth by the influence of water.

INTRODUCTION

Enstatite (E) chondrites are highly reduced meteorites that mainly consist of Mg-pyroxene (enstatite), metal (kamacite), and Fe sulfide (troilite). The enstatite contains only very low abundances of FeO, and the kamacite exhibits relatively high Si concentrations. Both characteristics are a consequence of low O_2 fugacities during condensation and accretion. Due to the reducing conditions in the region of formation several unusual minerals like phosphides, sulfides and nitrides are integrated into E chondrites (*e.g.*, Keil, 1989, and references therein).

With respect to the iron content, two subgroups can be distinguished: EH chondrites (with H for high iron) and EL chondrites (with L for low iron) (*e.g.*, Sears, 1980; Sears *et al.*, 1982; Hertogen *et al.*, 1983; Weeks and Sears, 1985; Kallemeyn and Wasson, 1986). According to the classification scheme of Van Schmus and Wood (1967), E chondrites include all petrologic types from 3 to 7. However, other authors have suggested an additional differentiation scheme based on mineralogical aspects. They define four mineralogical types to account for discrepancies between texture and mineralogy found in many E chondrites (Zhang *et al.*, 1995). Because of these differences and relatively large variations in the chemical composition, the classification of E-chondritic samples turns out to be more difficult than that of ordinary chondrites. Hence, reclassifications are not unusual (*e.g.*, Kallemeyn and Wasson, 1986; Zhang *et al.*, 1995; Lin and Kimura, 1997; Rubin and Scott, 1997; Rubin *et al.*, 1997).

First noble gas analyses of an E chondrite (Abee) were carried out by Begemann *et al.* (1959) as well as by Zaehringer and Gentner (1960) (see also Wacker and Marti, 1983). Crabb and Anders (1981, 1982) gave the first systematic investigation of noble gases in several E chondrites. Since then, numerous new samples have been recovered on blue ice fields in Antarctica and also in some hot deserts, especially the Sahara. Recently, Okazaki *et al.* (1998) have published measurements of noble gases of 11 E chondrites mainly from the Japanese Antarctic meteorite collection. We have investigated the noble gas record (elemental concentrations and isotopic ratios) of 43 E-chondritic meteorites with unknown gas contents and remeasured 14 samples, for which rare gas data already existed (see Schultz and Franke, 2000). Table 1 gives more information on the sample suite examined in this paper.

Altogether, the noble gas inventories of 62 E chondrites have been published so far (including this work). This is a considerable number in comparison to the total number of known E chondrites. Correcting for pairing and taking into

TABLE 1. List of analysed enstatite chondrites with measured noble gas concentrations and $^{129}Xe/^{132}Xe$ ratios.

Sample	Type	Provided by	$^{3}He^{\$}$	$^{4}He^{\$}$	$^{20}Ne^{\$}$	$^{21}Ne^{\$}$	$^{22}Ne^{\$}$	$^{36}Ar^{\$}$	$^{38}Ar^{\$}$	$^{40}Ar^{\$}$	$^{84}Kr^{\dagger}$	$^{132}Xe^{\dagger}$	$^{129}Xe/^{132}Xe$
1. Abee[#,&,§]	EH4 m.b.*	MPI Mainz	12.1	1123	3.75	2.93	3.30	36.3	7.11	5547	1590	1150	5.19
2. Acfer287[&]	E4*	Univ. of Münster	30.0	687	4.61	4.48	5.57	1.24	0.30	3770	221	140	7.02
3. ALH 84170[#]	EH3*	NASA, Houston	153	274 000	1220	14.6	108	58.5	12.0	5215	2705	6690	1.28
4. ALH 84206[#]	EH3*	NASA, Houston	71.6	112 750	580	13.0	57.9	41.3	8.73	5665	2605	5740	1.34
5. ALH 85119[#]	EL3*	NASA, Houston	28.4	77 950	1560	4.87	124	82.4	15.6	4405	2770	6730	1.15
6. ALH 88046[#]	EH3*	MPI Mainz	64.2	46 270	169	10.8	24.2	27.1	6.14	3650	3080	7050	1.22
7. ALH 88070[#]	EH3*	MPI Mainz	64.8	24 570	87.9	11.0	18.0	17.4	4.47	3230	2580	5650	1.31
8. Atlanta[#,&]	EL6*	MPI Mainz	52.6	1008	10.4	11.2	12.0	4.14	1.42	4875	280	168	6.61
9. DaG 734[#]	EL4‡	MPI Mainz	26.5	932	8.15	5.57	6.73	10.3	2.11	5262	2723	270	1.86
10. Eagle[#,§]	EL6*	Nat. Hist. Museum, London	47.5	987	8.93	9.48	10.5	14.9	3.64	5330	906	590	3.52
11. EET 83322[#]	EH3*	NASA, Houston	38.5	1150	7.58	6.14	7.14	11.8	2.79	3460	3145	3760	1.30
12. EET 87746[#]	EH3@	NASA, Houston	0.68	975	3.48	0.14	0.55	37.4	7.00	11 215	25 700	34 600	1.02
13. EET 90102[#]	EL6*	NASA, Houston	12.1	930	20.6	4.44	7.14	387	74.3	3303	10 940	4130	1.37
14. EET 90299[#]	EL3*	NASA, Houston	39.9	167	6.59	6.79	7.78	4.09	1.51	1943	1989	4008	1.11
15. EET 92063[#]	EL6*	NASA, Houston	56.8	607	9.87	8.78	10.0	91.2	18.4	4833	2920	1090	3.56
16. EET 96103[#]	EH4*	NASA, Houston	6.11	949	2.02	0.80	1.08	52.9	10.2	5347	1660	1880	1.65
17. EET 96135[#]	EH4/5*	NASA, Houston	5.37	828	1.90	0.77	1.03	53.0	10.2	5050	1545	1730	1.70
18. EET 96299[#]	EH4/5*	NASA, Houston	6.53	1006	2.10	0.82	1.11	53.6	10.4	5470	1717	2050	1.60
19. Forrest 033	EL6*	MPI Mainz	33.3	692	17.4	11.8	13.0	83.5	16.2	3450	2120	664	2.72
20. Galim b[#]	EH3@	Mus. Nat. D'Hist. Nat., Paris	0.06	886	0.58	0.02	0.08	4.77	0.89	6713	615	497	3.23
21. Grein 002[#,§]	EL4/5*	MPI Mainz	56.4	1315	11.3	9.39	11.1	126	25.0	7900	6300	3060	2.73
22. GRO 95517[#]	EH3*	NASA, Houston	54.5	1133	10.3	9.71	11.1	7.34	2.46	4622	2674	3809	1.34
23. GRO 95626[#]	EL6*	NASA, Houston	35.0	880	5.99	4.97	6.17	37.9	7.72	5460	1447	525	4.36
24. Happy Canyon[&]	EL6 m.b.**	MPI Mainz	42.4	412	8.54	8.96	10.6	2.45	0.91	3040	203	246	6.32
25. Hvittis[#,&,§]	EL6*	MPI Mainz	30.8	1413	8.21	8.10	8.80	60.2	12.2	4130	1580	1010	2.62
26. Ilafegh 009[#,&,§]	EL7 m.r.*	Univ. of Münster	6.26	221	3.69	3.62	3.92	2.58	0.83	3350	178	147	3.69
27. Indarch[#,&,§]	EH4*	MPI Mainz	12.8	347	4.45	3.66	4.22	6.23	1.56	6160	1190	945	3.75
28. KaidunIV[&]	EL3*	Vernadsky Institute, Moscow	0.79	530	1.00	0.31	0.41	8.40	1.60	4094	1158	1440	1.36
29. Kota-Kota[#,&]	EH3*	Nat. Hist. Museum, London	56.6	1030	8.96	8.37	9.63	7.25	2.41	4515	998	1110	1.93
30. LEW 87119[#]	EL6*	NASA, Houston	9.98	630	4.19	2.85	3.31	73.5	14.2	2975	3055	1100	3.21
31. LEW 88714[#]	EL6*	NASA, Houston	10.4	689	3.51	2.62	2.93	72.0	13.7	2370	3120	1100	3.08
32. LEW 87223[#,§]	E3 an*	NASA, Houston	13.9	1062	2.43	1.83	2.18	3.15	0.90	4000	577	319	3.75
33. LEW 88180[#]	EH5*	NASA, Houston	31.8	1173	7.83	4.30	5.64	130	25.4	5745	5360	1810	1.97
34. LON 94100[#,§]	EL6*	NASA, Houston	52.0	920	8.42	8.40	9.65	31.8	6.80	5130	1130	582	4.64
35. MAC 88136[#]	EL3*	NASA, Houston	42.6	1237	982	3.60	80.9	48.0	9.30	4322	1770	2240	1.46
36. PCA 82518[#]	EH3*	NASA, Houston	4.69	795	1.42	0.66	0.87	6.15	1.24	5450	2174	1420	1.83
37. PCA 91020[#]	EL3*	NASA, Houston	41.1	203	10.5	9.53	10.6	6.63	2.18	1183	1498	1539	1.87
38. Pillistfer[#,&,§]	EL6*	MPI Mainz	6.61	766	2.64	2.13	2.33	24.9	4.80	5370	1350	779	2.15
39. Qingzhen[#,&,§]	EH3*	MPI Mainz	2.98	230	3.60	2.65	2.98	7.87	1.72	1620	1240	1280	1.94
40. QUE 93372[#]	EL3*	NASA, Houston	90.9	1384	16.5	17.2	19.2	25.9	6.32	4495	1455	531	5.12
41. QUE 93351[#]	EL3*	NASA, Houston	43.4	1558	8.15	7.76	9.23	7.46	1.73	4788	1116	1185	1.93
42. QUE 94594[#]	EH5*	NASA, Houston	47.4	1479	8.63	8.06	9.46	8.49	2.22	5600	1426	1495	1.87
43. QUE 94204[#]	EH7 m.r.*	NASA, Houston	66.4	731	15.1	16.5	17.6	8.16	2.21	3140	554	337	1.17
44. QUE 97462[#]	EL6*	NASA, Houston	7.78	1850	12.8	1.75	3.19	211	40.7	5583	5504	2261	1.55
45. RKPA80259[#]	EH5*	NASA, Houston	38.9	1140	8.69	5.35	6.76	107	20.8	4100	3670	1450	1.86
46. SAH 97096[#,§]	EH3*	Univ. of Münster	14.3	330	7.21	6.59	7.14	8.11	2.14	1340	2735	1900	1.89
47. SAH 97166[#]	EH3*	Univ. of Münster	11.9	185	7.93	6.86	7.58	12.1	3.02	2288	3086	1765	2.01
48. St. Marks[#,&]	EH5*	MPI Mainz	1.09	304	1.33	0.27	0.41	38.0	7.12	4705	1645	697	3.68
49. Tanezrouft 031	EL5*	Univ. of Münster	2.07	342	1.65	1.44	1.64	59.7	11.4	3420	2840	1220	2.25
50. TIL 91714[#]	EL5*	NASA, Houston	2.49	647	3.62	0.71	1.00	80.8	15.4	5068	1986	836	2.56

TABLE 1. *Continued.*

Sample	Type	Provided by	^{3}He$^{\$}$	^{4}He$^{\$}$	^{20}Ne$^{\$}$	^{21}Ne$^{\$}$	^{22}Ne$^{\$}$	^{36}Ar$^{\$}$	^{38}Ar$^{\$}$	^{40}Ar$^{\$}$	^{84}Kr†	^{132}Xe†	^{129}Xe/^{132}Xe
51. Y-691#,&	EH3*	NIPR, Tokyo	2.78	424	3.18	0.84	1.22	22.6	4.36	1675	3170	7280	1.18
52. Y-74370#	EH3††	NIPR, Tokyo	2.32	588	1.32	0.47	0.63	6.23	1.21	5585	1355	1200	2.02
53. Y-791790#	EH4‡‡	NIPR, Tokyo	3.44	829	3.14	1.01	1.32	143	27.2	6285	2820	718	3.77
54. Y-791810#	EH4‡‡	NIPR, Tokyo	3.07	632	3.15	1.05	1.39	137	26.1	6200	2840	722	3.86
55. Y-792959#	EH3*	NIPR, Tokyo	34.5	746	8.12	7.07	8.30	8.38	2.11	1730	2170	2840	1.24
56. Y-793225#	E6 an§§	NIPR, Tokyo	54.4	1025	9.86	9.65	11.6	60.9	12.3	5990	1925	714	4.51
57. Y-8404#	EH6##	NIPR, Tokyo	10.7	797	1.80	1.68	2.00	0.81	0.32	5301	92.3	75.0	9.70

$^{\$}$In 10^{-8} ccSTP/g.
†In 10^{-12} ccSTP/g.
#Average values of two or more analyses (He and Ne data of experimentally weathered samples are integrated, too).
§Samples selected for the weathering experiment.
&For previous noble gas analyses see Schultz and Franke (2000).
*MetBase (1999).
‡Grossman (2000).
@Kong *et al.* (1997).
**Keil (1989).
††per. comm. A. El Goresy (2000).
‡‡Kimura and Lin (1999).
§§Okazaki *et al.* (1998).
##Lin and Kimura (1997).
Abbreviations: m.b. = melt breccia, m.r. = melt rock, an = anomalous.

account only specimens of >5 g, MetBase (1999) lists less than 90 individual falls and finds.

The noble gas content of a meteorite consists of different gas components, which are defined by distinct elemental and isotopic compositions (*e.g.*, Ozima and Podosek, 1983). In this paper, which represents an expanded and updated version of previous short communications (Patzer and Schultz, 1999; Patzer *et al.*, 1999), we focus on cosmogenic and radiogenic noble gas nuclides. The composition and distribution of trapped rare gases of E chondrites will be discussed in a second paper (Patzer and Schultz, unpubl. data).

Cosmogenic noble gases are used to determine cosmic-ray exposure ages as well as to obtain information on the collisional history of the meteorite parent body (*e.g.*, Cressy and Bogard, 1976; Nishiizumi *et al.*, 1980; Schultz and Freundel, 1985; Eugster, 1988; Schultz *et al.*, 1991). In particular, we address the following questions: (1) Is the cosmic-ray exposure age distribution of E-chondrite subgroups the same and how does the cosmic-ray exposure age distribution of E chondrites compare to the ordinary chondrite groups? (2) Does there exist a systematic trend between exposure age and petrologic type? (3) What percentage of E chondrites are regolith breccias?

EXPERIMENTAL PROCEDURE AND RESULTS

The concentrations and isotopic compositions of noble gases were determined with an all-metal mass spectrometer (MAP215 manufactured by Mass Analyser Products) using a magnetic sector field of 90° and a so-called extended geometry. For the gas extraction, a tungsten crucible with a double vacuum was available and heated in one step to ~1800 °C. The purification of the rare gases was sequentially performed by means of a titanium and a zirconium-aluminum getter. In order to avoid interference, the purified noble gas amount was finally split into at least two fractions using temperature-controlled charcoal. Sample preparation, experimental procedure and corrections are given by Scherer *et al.* (1998) (see also Loeken *et al.*, 1992).

The noble gas data of all analyzed samples are compiled in Table 1. The relative uncertainties of the determined gas concentrations vary from 5 to 10% for He, Ne, and Ar and from 10 to 15% for Kr and Xe. All isotopic ratios are known to better than 1%, except for Xe (10%). The uncertainty includes statistical errors, errors of mass discrimination, background, and interference corrections. Background concentrations of He as well as of Kr and Xe principally ranged below 5% of the respective gas amount in the sample, of Ne below 1.5%, and of Ar below 2%. For He, Kr and Xe a fractionation correction has been applied. We determined average mass fractionation factors caused by the spectrometer of 0.55%/amu for Kr and 0.3%/amu for Xe. The correction factor for the ^{3}He/^{4}He ratio varied between 1.126 and 0.952. Mass fractionation for Ne and Ar was negligible. Another correction was related to the interference of water molecules and doubly charged ions with the quantitative determination of ^{20}Ne and ^{22}Ne. Applied factors amounted to 0.6% of mass 18 for mass 20 due to $^{1}H_2{}^{18}O$, 0.3% of mass 40 for mass 20 due to $^{40}Ar^{++}$, and 8% of mass 44 for mass 22 due to $(^{12}C^{16}O_2)^{++}$.

To evaluate cosmic-ray exposure ages and gas retention ages, methods were used as described in Scherer *et al.* (1998). We calculated production rates for cosmogenic ^{3}He, ^{21}Ne, and ^{38}Ar (P^3, P^{21}, P^{38}) and cosmic-ray exposure ages on the basis of the cosmogenic ^{22}Ne/^{21}Ne ratio as shielding parameter according to Eugster (1988). The production rate of ^{38}Ar, however, was reduced by 13% (Schultz *et al.*, 1991):

$$P^3 = F\,[2.09 - 0.43(^{22}\mathrm{Ne}/^{21}\mathrm{Ne})_c]$$

$$P^{21} = 1.61F\,[21.77(^{22}\mathrm{Ne}/^{21}\mathrm{Ne})_c - 19.32]^{-1}$$

$$P^{38} = F\,[0.125 - 0.071(^{22}\mathrm{Ne}/^{21}\mathrm{Ne})_c]$$

As the determination of cosmic-ray exposure ages is based on L-chondritic chemistry, appropriate E-chondritic chemical correction factors F were needed. We evaluated these factors according to the following equations on the basis of four different chemical groups as published by Kong *et al.* (1997). Additionally required elemental data not given in Kong *et al.* (1997) were adopted from Mason (1979):

$$[^3\mathrm{He_c}] = 0.0174\{\mathrm{Ti + Cr + Mn + Fe + Ni}\} + 0.0266(100 - \{\mathrm{Ti + Cr + Mn + Fe + Ni}\}) \text{ in wt\%}$$
(Cressy and Bogard, 1976)

$$[^{21}\mathrm{Ne_c}] = 1.63\{\mathrm{Mg}\} + 0.6\{\mathrm{Al}\} + 0.32\{\mathrm{Si}\} + 0.22\{\mathrm{S}\} + 0.07\{\mathrm{Ca}\} + 0.021\{\mathrm{Fe + Ni}\} \text{ in weight fractions}$$
(Schultz and Freundel, 1985)

$$[^{38}\mathrm{Ar_c}] = 2.6\{\mathrm{K}\} + 1.58\{\mathrm{Ca}\} + 0.33\{\mathrm{Ti + Cr + Mn}\} + 0.086\{\mathrm{Fe + Ni}\} \text{ in weight fractions}$$
(Schultz *et al.*, 1991)

Correction factors F for EH3 chondrites resulted to be 0.97, 0.77, and 1.00 for ^{3}He, ^{21}Ne, and ^{38}Ar exposure ages, respectively, for EH4–6 chondrites 0.97, 0.79, and 0.99, for EL3 + 4 chondrites 0.98, 0.87, and 1.02, and for EL5 + 6 1.00, 0.94, and 0.89.

In Table 2, cosmogenic and radiogenic isotope abundances as well as calculated cosmic-ray exposure ages are listed. The uncertainty for ^{21}Ne exposure ages (T_{21}) is estimated to be 20%. This value takes into account significant variations in the chemical composition of E chondrites (*e.g.*, Kong *et al.*, 1997). For all statistical evaluations, we refer to T_{21} only because ^{3}He exposure ages can be affected by diffusive loss due to moderate solar heating on orbits with small perihelia (Hintenberger *et al.*, 1966; Schultz and Weber, 1995, 1997). On the other hand, T_{38} may show higher uncertainty for samples with high amounts of trapped Ar. In these cases, the determination of the cosmogenic Ar concentration turns out to be difficult due to the possible discrepancy between the assumed ^{36}Ar/^{38}Ar ratio of 5.32 and its real but unknown value. In addition, cosmogenic ^{38}Ar is more likely to be influenced (depleted) by terrestrial weathering than ^{21}Ne and ^{3}He (Gibson and Bogard, 1978; Scherer *et al.*, 1994). Consequently, we consider T_{21} as the most reliable.

The U/Th-He (T_4) and K/Ar (T_{40}) gas retention ages (Table 2) were calculated assuming that the average concentrations of U, Th and K in E chondrites are 10 ppb, 34 ppb and 800 ppm, respectively (Mason, 1979).

DISCUSSION

Shielding Conditions and Diffusive Loss of Helium-3

Diffusive loss of ^{3}He, which is essentially of cosmogenic origin in most meteoritic samples, can be identified in the so-called Bern plot (Fig. 1; Eberhardt *et al.*, 1966; Nishiizumi *et al.*, 1980). This diagram shows the cosmogenic ^{3}He/^{21}Ne ratio (^{3}He/^{21}Ne)$_c$ as a function of cosmogenic ^{22}Ne/^{21}Ne (^{22}Ne/^{21}Ne)$_c$. The latter ratio is widely used as a shielding parameter for production rates and thus for the determination of cosmic-ray exposure ages (*e.g.*, Nishiizumi *et al.*, 1979; Reedy, 1985; Eugster, 1988). A sensible correction for shielding, however, is only possible within the range of $1.08 <$ (^{22}Ne/^{21}Ne)$_c$ < 1.20 (*e.g.*, Leya *et al.*, 2000). For lower ratios, production rates exhibit considerable variations and for larger values, a contribution induced by solar cosmic rays is possible. The Bern line represents a best fit through ordinary chondrite data. Due to changing radii and sample positions (*i.e.*, shielding conditions) the position of individual data points may vary within ±15%. Meteorites falling considerably below this range have experienced diffusive loss of ^{3}He or its precursor, tritium.

Many E chondrites as well as lodranites (Weigel *et al.*, 1999) do not follow the Bern line but scatter over a wide range of both, (^{3}He/^{21}Ne)$_c$ and (^{22}Ne/^{21}Ne)$_c$. Hence, any information about the shielding conditions of these meteorites and ^{3}He losses has to be considered carefully. For the cases in question, the scattering of data points is probably due to high chemical variations as compared to ordinary chondrites (*e.g.*, Kong *et al.*, 1997). The average abundances of relevant target elements of ^{3}He$_c$ and ^{21}Ne$_c$ often differ significantly from L-chondritic values. On one hand, Fe and Ni contents of E chondrites are higher and lead to lower ^{3}He$_c$ concentrations. On the other, Mg and Al as main target elements of ^{21}Ne$_c$ are less abundant in E chondrites so that less ^{21}Ne$_c$ is produced. The net results are relatively higher (^{3}He/^{21}Ne)$_c$ ratios in E chondrites. This is illustrated in Fig. 2. Three E-chondritic samples were corrected for the relevant L-chondritic elemental abundances and projected into the Bern plot in order to demonstrate the dependence of cosmogenic production rates and the related shielding situation on the chemical composition.

The Calculation of Production Rates by Means of Individual and Average Chemical Data—A Comparison

For the calculation of production rates of cosmogenic nuclides, parameters like the shielding position and chemical

TABLE 2. Cosmogenic and radiogenic noble gas concentrations, cosmic-ray exposure ages and gas retention ages of enstatite chondrites.

Sample	$^{3}He_{c}$	$^{4}He_{r}$	$^{21}Ne_{c}$	$^{38}Ar_{c}$	$^{40}Ar_{r}$	$(^{22}Ne/^{21}Ne)_{c}$	T_3	T_{21}	T_{38}	T_4	T_{40}
Abee	12.1	1052	2.93	0.33	5447	1.091	7.7	10.0	8.2	3.61	4.07
Acfer 287	30.0	507	4.48	0.080	3770	1.243	19.8	26.2	2.5	1.97	3.92
ALH 84170 + 84206	49.3	–	11.6	1.23	–	1.099	31.5	43.2	30.0	–	–
ALH 85119	2.67	–	0.79	0.28	–	1.110	1.7	2.7	6.8	–	–
ALH 88046 + 88070	52.7	–	10.6	1.33	–	1.067	33.3	33.4	31.0	–	–
Atlanta	52.6	692	11.3	0.74	4875	1.067	32.3	29.0	19.5	2.50	4.17
DaG 734	26.5	773	5.57	0.20	5262	1.161	16.7	21.8	6.0	2.80	4.23
Eagle	47.5	702	9.48	0.97	5250	1.106	29.4	29.9	27.5	2.53	4.24
EET 83322	38.5	915	6.13	0.65	3460	1.136	24.8	26.7	16.9	3.12	3.81
EET 87746	0.68	971	0.13	0.027	11 215	1.110	0.44	0.50	0.67	3.26	4.86
EET 90102	12.1	857	4.36	1.86	3303	1.280	7.8	24.6	70.3	2.98	3.78
EET 90299	39.9	–	6.79	0.85	1943	1.146	25.5	27.1	21.8	–	3.27
EET 92063	56.8	267	8.77	1.49	4833	1.122	35.3	29.6	42.3	1.05	4.16
EET 96103 + 96135 + 96299	6.11	912	0.79	0.33	5347	1.211	4.0	4.4	9.9	3.11	4.06
Forrest 033	33.3	493	11.8	0.53	3450	1.038	20.2	25.6	13.3	1.91	3.83
Galim b	0.062	886	0.018	0.004	6713	1.110	0.040	0.068	0.088	3.06	4.48
Grein 002	56.4	977	9.37	1.42	6705	1.171	36.6	44.1	39.3	3.21	4.28
GRO 95517	54.5	807	9.71	1.24	4622	1.137	35.1	42.3	32.0	2.99	4.10
GRO 95626	35.0	669	4.95	0.65	5460	1.230	22.4	24.3	22.1	2.34	4.28
Happy Canyon	42.4	158	8.96	0.51	3040	1.178	26.8	37.4	15.9	0.82	3.71
Hvittis	30.8	1228	8.11	1.01	4130	1.085	18.9	21.8	27.3	3.75	4.01
Ilafegh 009	6.26	183	3.63	0.40	4373	1.074	3.8	9.4	10.5	0.76	4.05
Indarch	12.8	270	3.66	0.45	5675	1.127	8.2	14.9	11.7	1.11	4.12
Kaidun IV	0.79	526	0.31	0.03	4094	1.177	0.5	1.4	0.7	2.04	4.00
Kota-Kota	56.6	691	8.36	1.19	4515	1.141	36.5	37.1	31.2	2.51	4.03
LEW 87119 + 88714	10.2	598	2.73	0.35	2673	1.084	6.3	8.0	8.8	2.26	3.57
LEW 87223	13.9	978	1.83	2.91	5532	1.152	8.9	7.5	9.2	3.27	4.13
LEW 88180	31.4	939	4.19	1.06	5570	1.240	20.8	25.1	32.7	3.17	4.14
LON 94100	52.0	609	8.39	0.95	5056	1.156	32.6	31.1	28.7	2.28	4.20
MAC 88136	1.95	–	1.14	0.42	4460	1.110	1.2	3.9	10.2	–	4.08
PCA 82518	4.69	767	0.66	0.093	5450	1.198	3.1	3.6	2.7	2.75	4.28
PCA 91020	41.1	–	9.53	1.06	1183	1.092	25.9	30.2	25.2	–	2.80
Pillistfer	6.61	726	2.13	0.14	5313	1.047	4.1	5.3	3.7	2.61	4.25
Qingzhen	2.98	212	2.65	0.27	1930	1.080	1.9	8.9	6.5	0.89	3.24
QUE 93351 + 94594	45.0	1256	7.88	0.51	5113	1.175	29.0	35.1	13.7	3.89	4.21
QUE 93372	90.9	838	17.2	1.63	4776	1.109	58.1	66.2	41.2	2.88	3.92
QUE 94204	66.4	333	16.5	0.78	3140	1.062	41.9	49.0	18.2	1.39	3.54
QUE 97462	7.47	1697	1.71	1.20	5593	1.110	4.7	5.5	33.6	4.37	4.31
RKPA80259	38.9	905	5.33	0.92	4100	1.206	25.5	29.0	27.2	3.07	3.80
SAH 97096 + 97166	14.3	244	6.59	0.71	1328	1.063	9.0	20.2	16.4	1.00	2.90
St. Mark's	1.09	298	0.27	0.044	4705	1.205	0.68	1.0	1.1	1.23	3.94
Tanezrouft 031	2.07	330	1.44	0.21	3420	1.115	1.3	4.7	5.9	1.32	3.82
TIL 91714	2.36	392	0.74	0.31	5010	1.052	1.4	1.7	8.0	1.57	4.20
Y-691	2.78	408	0.83	0.14	1675	1.258	1.9	5.4	4.6	1.63	3.08
Y-74370	2.32	574	0.47	0.043	5585	1.179	1.5	2.4	1.2	2.18	4.30
Y-791790 + 791810	3.25	711	1.02	0.41	6243	1.155	2.1	4.7	11.2	2.34	4.22
Y-792959	34.5	539	7.05	0.62	1730	1.159	22.4	33.5	16.4	2.06	3.16
Y-793225	54.4	700	9.64	0.95	5990	1.199	35.1	46.8	29.2	2.56	4.37
Y-8404	10.8	774	1.68	0.19	5300	1.189	7.0	8.6	5.5	2.72	4.06

Abbreviations: c = cosmogenic, r = radiogenic. All concentrations in 10^{-8} ccSTP/g. T_3, T_{21}, T_{38} = cosmic-ray exposure ages calculated with cosmogenic ^{3}He, ^{21}Ne and ^{38}Ar. T_4, T_{40} = gas retention ages evaluated with radiogenic ^{4}He and ^{40}Ar.

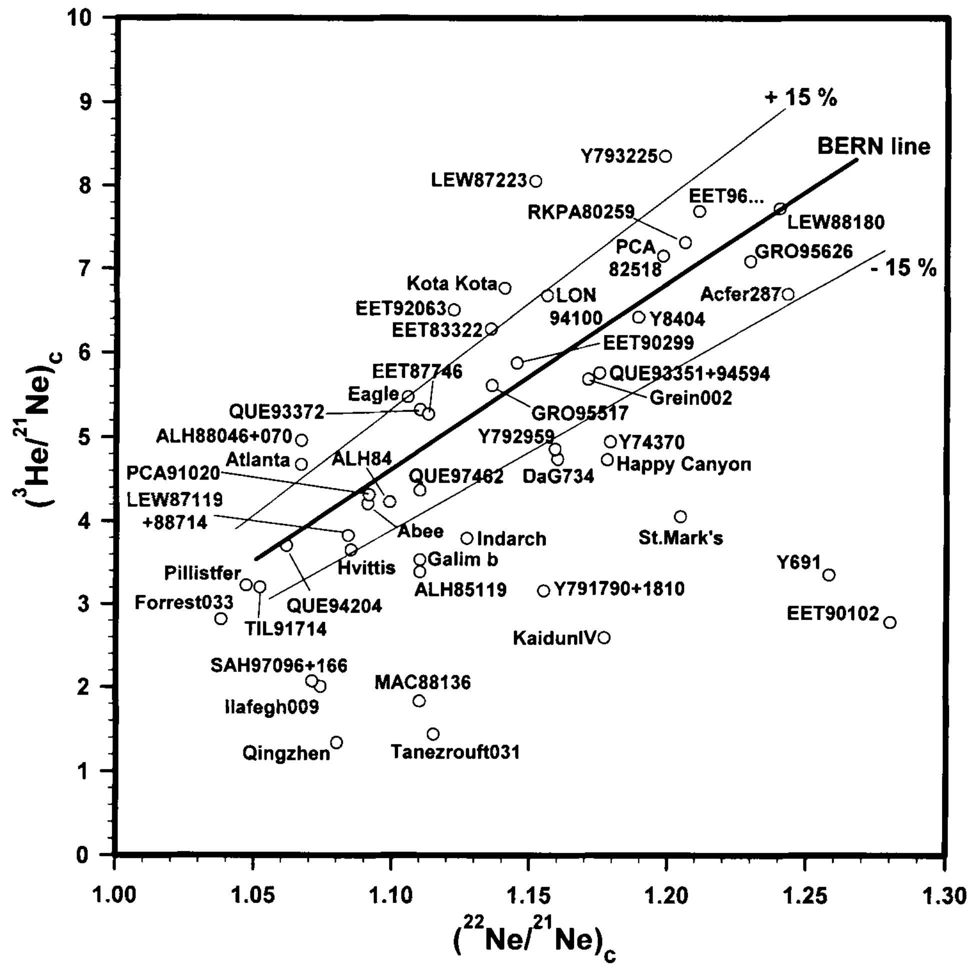

FIG. 1. Cosmogenic ^{3}He/^{21}Ne and ^{22}Ne/^{21}Ne ratios for enstatite chondrites. Undisturbed ordinary chondrites plot ±15% around a trend line ("Bern line"; Eberhardt *et al.*, 1966) while those with a ^{3}He deficit fall below this line. Enstatite chondrites scatter over a considerably wider range of values. This form of "diffuse" plotting is possibly due to relatively large variations in chemical composition. Hence, the use of the Bern line for shielding corrections for E chondrites is limited as compared to ordinary chondrites.

composition of the meteorite have to be taken into account (Eugster, 1988; see also Michel *et al.*, 1997; Leya *et al.*, 2000). Generally, the (^{22}Ne/^{21}Ne)$_c$ is applied to correct for shielding. Chemical correction factors are adopted in order to account for compositional differences of a meteorite class from L-chondritic chemistry (see above). We determined the production rates of cosmogenic ^{3}He, ^{21}Ne, and ^{38}Ar with average chemical data for four different E-chondritic groups (Kong *et al.*, 1997). We also considered production rates for ^{21}Ne$_c$ on the basis of the individual chemical composition as far as literature data were available.

In Fig. 3, we visualized the ratios of individual to average chemical correction factors of 28 samples, for which the chemical composition was known. Most factors calculated with individual elemental abundances (F_i) vary from those basing on average group concentrations (F_a) within about ±10%. Only for five samples, the individual factors are observed to be >10% lower than F_a. Overall, a systematic trend becomes apparent: F_i for EH3 chondrites tends to be generally somewhat higher and for EL5 + 6 chondrites mostly lower than F_a. We decided to use F_a because individual chemical data may be less representative for the respective sample weights of <100 mg.

Pairing

Meteorites of one type that are found closely together and show striking similarities with respect to mineralogical and chemical parameters may be paired (*e.g.*, the Antarctic EH3 meteorites found at Pecora Escarpment or the Saharan EH3 finds recovered in 1997). Pairing is also proved by noble gas inventories and cosmic-ray exposure ages (*e.g.*, Schultz *et al.*, 1991; Benoit *et al.*, 2000). In order to be able to sensibly interpret the statistical distribution of cosmic-ray exposure ages of a given meteorite class, pairing has always to be considered.

For the investigated sample suite of 57 E chondrites, 7 new pairings are suggested based on chemical classification, noble gases, cosmic-ray exposure ages, and find locality

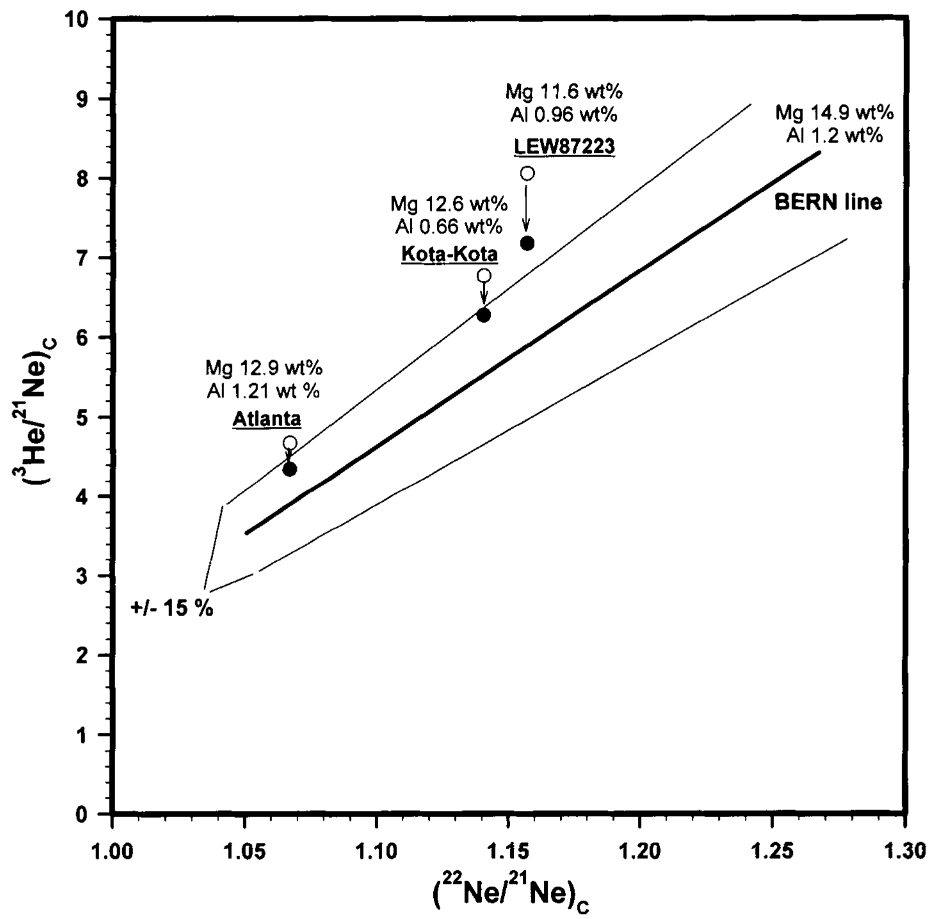

FIG. 2. Illustration of the influence of chemical composition on the position of E chondrites in the Bern plot. As an example, the individual chemical compositions of three E chondrites were corrected for L-chondritic elemental abundances (chemical composition from Atlanta: Mason, 1966; Kota-Kota: Easton and Elliott, 1977; Lewis Cliff 87223: Kong *et al.*, 1997; L chondrites: Jarosewich, 1990). Only Mg and Al were chosen because they represent the main target elements of cosmogenic ^{21}Ne. The elemental composition of L chondrites is 14.9 wt% Mg and 1.2 wt% Al. Since E chondrites generally contain less Mg and Al, their corrected cosmogenic ^{3}He/^{21}Ne ratios are lower.

(Table 3). The latter criterion may occasionally be a rather weak argument, especially for Antarctic meteorites, which can get separated in moving ice. Lewis Cliff (LEW) 87119 and LEW 88714, for example, were found in different years ~3 km apart. We consider them as fragments of the same meteoroid because of a similar classification and the similar noble gas record. Additionally, both E chondrites are of the same mineralogical type (Zhang *et al.*, 1995) and also show petrographical similarities (Mason, 1992).

The Distribution of Cosmic-Ray Exposure Ages of E Chondrites

In Fig. 4, the distribution of cosmic-ray exposure ages of E chondrites is illustrated in a semi-logarithmic vertical bar chart. The bar width corresponds to the uncertainty of age (20%). Most exposure ages range from 2 to 50 Ma. Only five samples plot below 2 Ma.

In general, the absolute cosmic-ray exposure age spectrum of E chondrites resembles that of ordinary chondrites (Fig. 4; Lipschutz and Schultz, 1999). This probably indicates that the parent bodies of both meteorite classes are located in similar parts of the solar system. Also, the exposure age systematics imply an at least as common number of collisional events for E chondrites as for ordinary chondrites (*e.g.*, Graf and Marti, 1989, 1991, 1992; Marti and Graf, 1992). However, the uncertainty of age of E chondrites is considerably larger than that of ordinary chondrites, which is essentially due to higher chemical heterogeneity. Additionally, a much smaller number of E-chondritic samples has been dated so far. Therefore, the resolution of clusters among the cosmic-ray exposure age of E chondrites proves to be more difficult. Clustering of cosmic-ray exposure ages (*e.g.*, at ~7 Ma for H chondrites; Fig. 4) is generally interpreted as a severe impact event on the meteorite parent body ejecting simultaneously many meteoroids. For E chondrites, three clusters at about 3.5, 8 and 25 Ma are detectable but further measurements are needed to confirm them.

With respect to EH and EL chondrites, no systematic trend can be observed (Fig. 4). Among the EL subgroup, however,

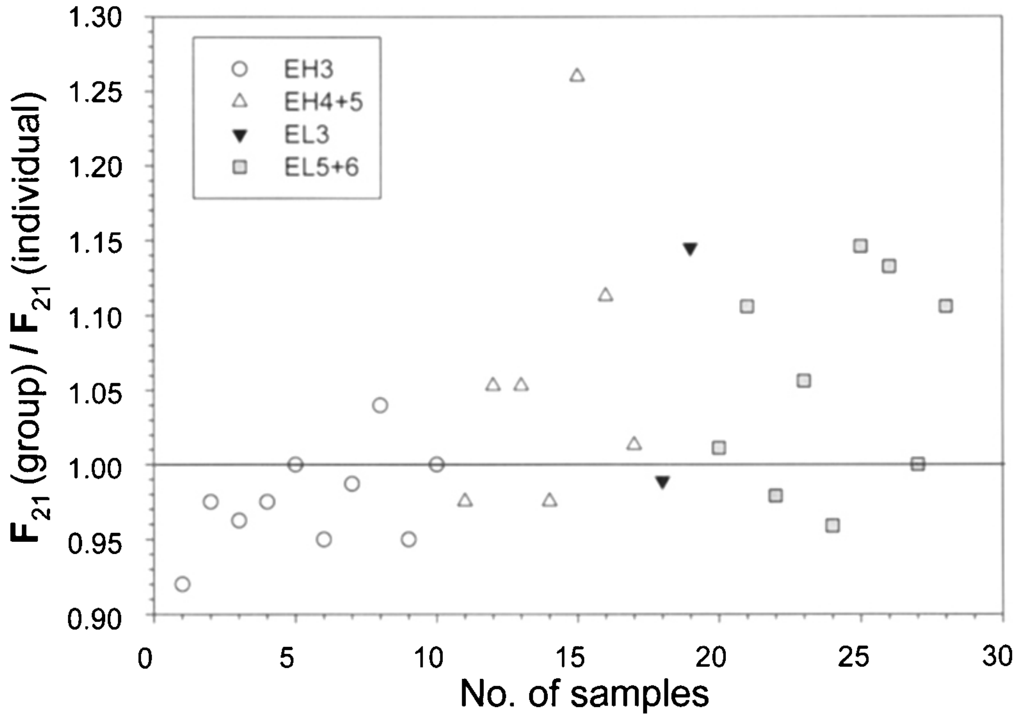

FIG. 3. Chemical correction factors for the calculation of cosmic-ray exposure ages can be determined considering either the average (F_{21}(group)) or individual (F_{21}(individual)) chemical composition. This figure compares correction factors for the calculation of cosmogenic ^{21}Ne exposure ages (T_{21}) evaluated with the average chemical composition of four different E-chondritic groups (Kong *et al.*, 1997) and individual compositions. We favor the usage of average factors assuming them to be more representative for sample weights of <100 mg.

TABLE 3. Paired samples.

Sample	Type	T_{21}	Find locality
ALH 84170	EH3	43.2	76°45'22" S 158°46'51" E
ALH 84206	EH3	43.1	76°45'51" S 158°45'55" E
ALH 88046	EH3	32.6	76°42'42" S 159°9'2" E
ALH 88070	EH3	34.1	76°42'39" S 159°9'1" E
EET 96103	EH4	4.2	approx. 76°11' S 157°10' E
EET 96135	EH4/5	4.5	approx. 76°11' S 157°10' E
EET 96299	EH4/5	4.5	approx. 76°11' S 157°10' E
QUE 93351	EL3	37.7	84°36'18" S 162°7'59" E
QUE 94594	EL3	34.4	approx. 84°S 168° E
LEW 87119	EL6	9.0	84°15'13" S 161°24'21" E
LEW 88714	EL6	7.0	84°16'28" S 161°21'19" E
Y-791790	EH4	4.3	approx. 71°30' S 35°40' E
Y-791810	EH4	5.0	approx. 71°30' S 35°40' E
SAH 97096	EH3	20.3	unknown coordinates
SAH 97166	EH3	23.1	unknown coordinates

many ages are found around or higher than 20 Ma (Fig. 5). Most samples of this age range belong to type EL6. Since the majority of EL chondrites is classified as type 6, the distribution may simply reflect a sample bias.

One of the samples with the shortest cosmic-ray exposure age we investigated is Galim b (0.068 Ma). This EH3 chondrite was found close to six nonweathered LL6-chondritic pieces (Galim a) in Cameroon in 1952 (Christophe-Michel-Lévy and Bourot-Denise, 1988). It has been suggested that both types correspond to one fall and that the Galim meteoroid represents a LL-chondritic polymict breccia with EH-chondritic clasts (Rubin, 1997). We have analyzed the noble gas inventories of both meteorites and found them to be identical within uncertainties. Thus, we support the suggestion that they fell together as a polymict breccia, which broke up during its passage through the atmosphere. The cosmic-ray exposure ages, which we have determined for both Galim lithologies, are comparatively short at 0.030 and 0.068 Ma, respectively. The difference of ages is significant though and can be explained by pre-irradiation of the EH clast before it became part of the LL-chondritic parent body regolith (Patzer *et al.*, 1999). This phenomenon of pre-irradiation has also been observed for other regolith breccias (Schultz *et al.*, 1972; Schultz and Signer, 1977; Lorin and Pellas, 1979).

A similar case is the unique breccia Kaidun with a variety of inclusions including EH and EL material (Ivanov *et al.*, 1984). We have measured Kaidun IV, an EL3 clast that also

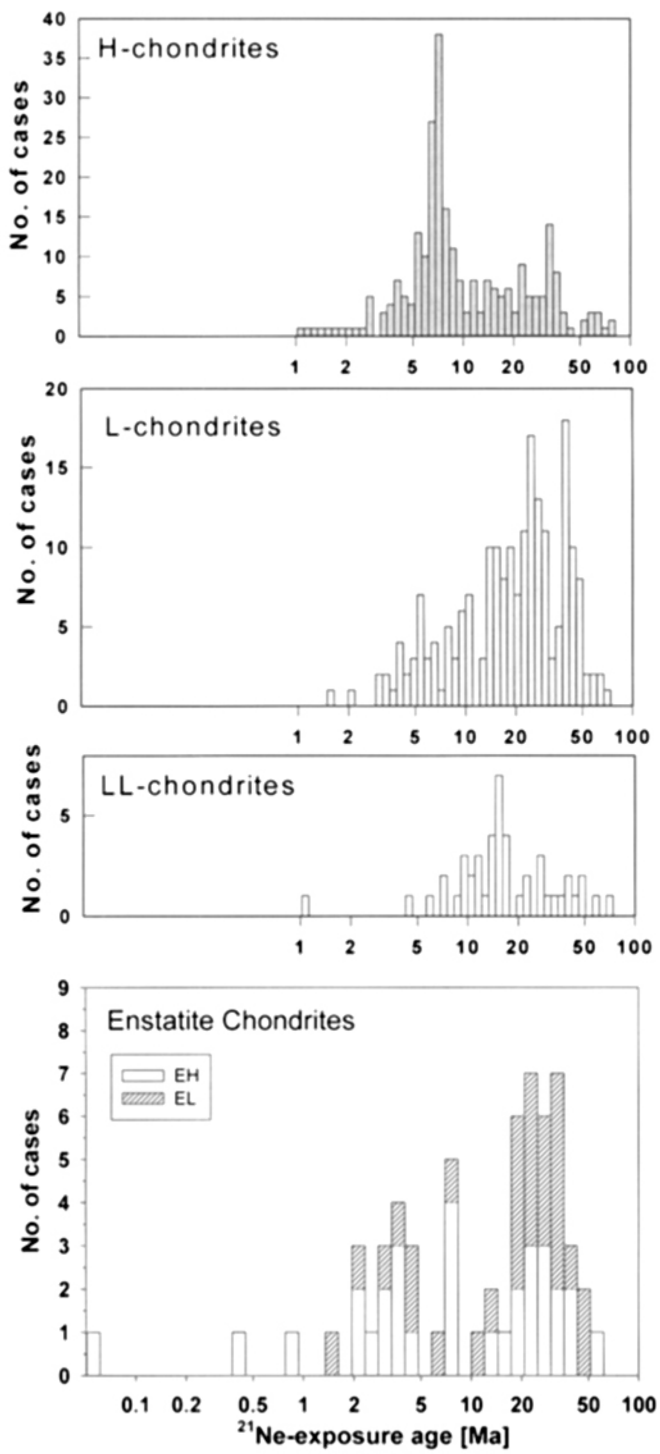

FIG. 4. Cosmic-ray exposure age distribution of ordinary chondrites (Lipschutz and Schultz, 1999; bar width corresponds to the uncertainty of age, which is 10%) and 61 EH and EL chondrites (this work and literature data, corrected for pairing). No systematic difference in the distribution patterns of the E-chondritic subgroups is apparent. Distinct clusters (*e.g.*, at 7 Ma for H chondrites) are interpreted as catastrophic impact events on the meteorite parent body. The uncertainty of cosmic-ray exposure ages of enstatite chondrites is estimated at 20% and, thus, significantly higher than that of ordinary chondrites. Consequently, the possible clusters at about 3.5, 8, and 20 Ma need to be confirmed.

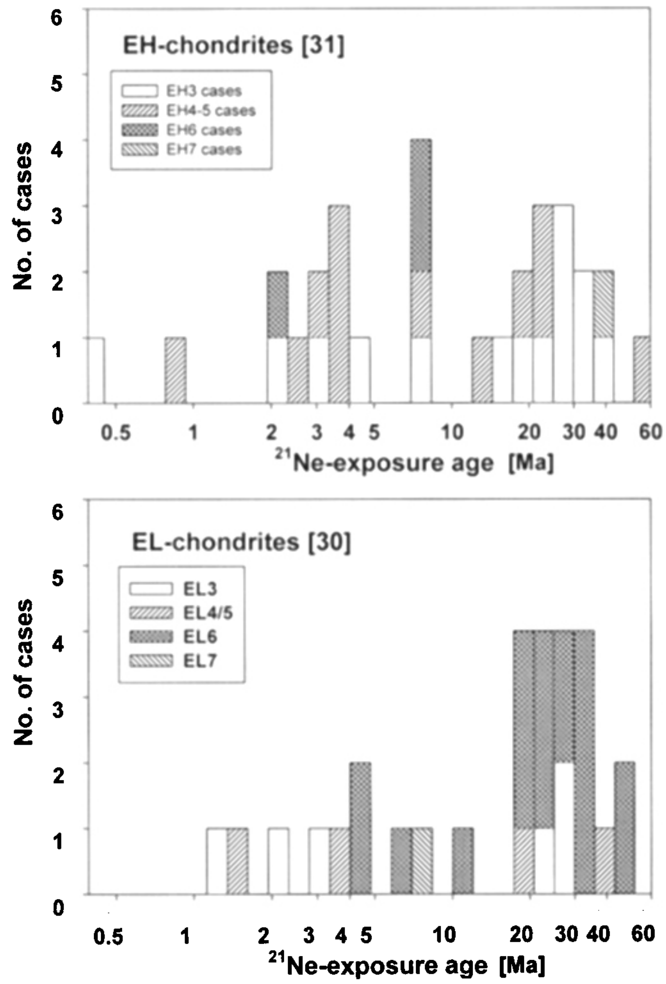

FIG. 5. Cosmic-ray exposure age distribution of individual petrologic types. For EL chondrites, the majority of samples classified as type EL6 yield cosmic-ray exposure ages around or higher than 20 Ma.

exhibits a rather short ^{21}Ne exposure age of ~1.4 Ma suggesting a complex irradiation history. However, further measurements are necessary to support this.

The other E chondrites of our sample suite that show low cosmic-ray exposure ages (<2 Ma) might be potential candidates for complex or multi-stage exposure to comic rays, too. Herzog *et al.* (1997) demonstrated that meteorites with short exposure ages tend to have complex irradiation histories and/or show deficits of ^{3}He due to solar heating (*e.g.*, St. Marks). Possible complex irradiation histories of meteorites are hard to detect from the noble gas inventory alone. Commonly, the determination of cosmogenic radionuclides is also needed.

Cosmic-ray exposure ages of <5 Ma are rare among ordinary chondrites. At first glance, this observation contradicts recent investigations of the dynamical lifetimes of objects in asteroid belt resonances. Assuming that chondrites are continuously delivered into main belt resonances, orbital simulations indicate that (1) by far most of the meteoroids are

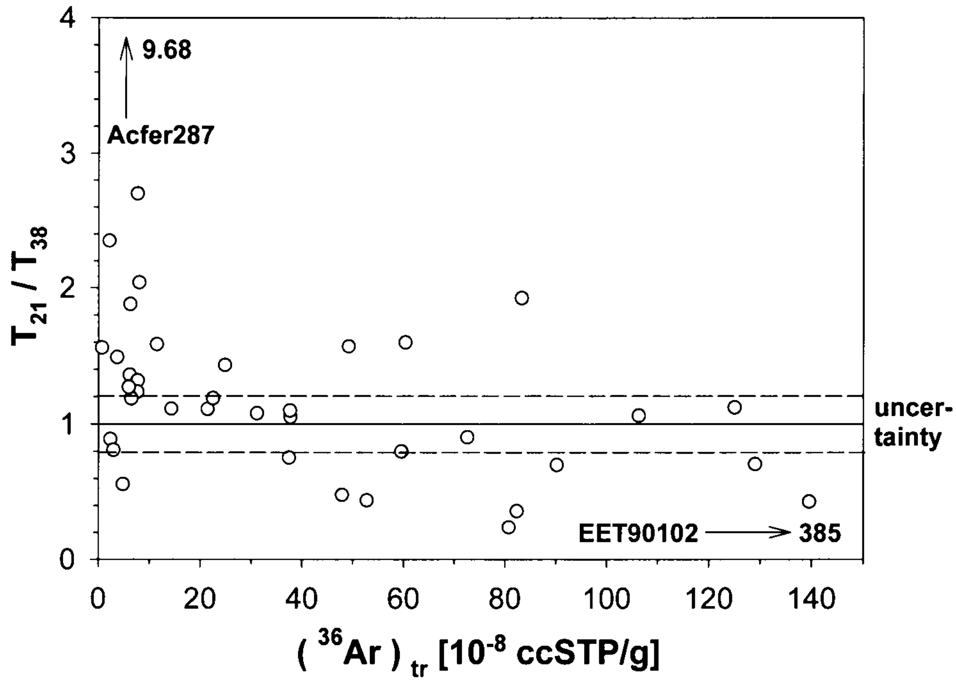

FIG. 6. The ratio of T_{21}/T_{38} as a function of trapped ^{36}Ar. In several cases, discrepancies between ^{21}Ne and ^{38}Ar exposure ages amount to more than 20%. For most samples with considerably lower T_{38}, the difference cannot be explained by high trapped Ar abundances. We suggest terrestrial weathering to be the cause for this phenomenon.

either lost in Jupiter- or Sun-crossing orbits or are driven out of the inner solar system and (2) those, which accidentally reach the region of the terrestrial planets, would have cosmic-ray exposure ages of <5 Ma (Gladman *et al.*, 1997; Morbidelli and Gladman, 1998). The difference between observed cosmic-ray exposure ages and calculated model cosmic-ray exposure ages implies that most meteorites acquired a considerable part of their exposure to cosmic rays in the main asteroid belt before entering the resonances and being brought to Earth relatively rapidly. The orbital evolution of these meteorites seems to be reflected best by an exposure history with a long first stage of irradiation (10 to 100 Ma) and a short second stage of <5 Ma.

A Comparison of T_{21} and T_{38}

In many cases, T_{21} and T_{38} of E chondrites differ significantly (>20%). One probable explanation for the discrepancy is the application of an inappropriate isotopic ratio for trapped Ar ($(^{36}Ar/^{38}Ar)_{tr}$), which critically influences the calculation of cosmogenic ^{38}Ar ($^{38}Ar_c$) (see also Eugster *et al.*, 1997). If trapped noble gas abundances are high and hence the cosmogenic fraction of ^{38}Ar relatively small, the absolute amount of $^{38}Ar_c$ is more likely to be miscalculated and results in a higher or lower T_{38}.

Some samples though show T_{38} being significantly lower than T_{21} and yet contain only small trapped gas amounts (Fig. 6). Consequently, these T_{21}/T_{38} ratios >1.2 can not be explained by insufficient correction for trapped Ar. We suggest that they lost cosmogenic ^{38}Ar due to alteration on Earth (Patzer and Schultz, 1999). The main target elements of $^{38}Ar_c$ production in E chondrites are Ca and Fe, which are present in kamacite (maximum 30 wt%), troilite (FeS, maximum 13 wt%), and oldhamite (CaS, maximum 2 wt%) as well as partly plagioclase (maximum 16 wt% with <10% anorthite). Especially oldhamite readily reacts with water. The dissolution and decomposition of both Ca- and metal-bearing minerals causes the loss of cosmogenic ^{38}Ar (see also Scherer *et al.*, 1994). Cosmogenic Ne, on the other hand, is mainly produced from Mg, which is found in minerals resistant to weathering effects. Hence, calculated T_{38} are shorter than T_{21}. The following paragraph discusses this subject in more detail.

An alternative explanation for reduced concentrations of $^{38}Ar_c$ in EH chondrites has been given by Graf and Marti (1992). Since EH chondrites exhibit Cl abundances of about an order of magnitude higher than those of ordinary chondrites these authors stated that the determined amount of trapped Ar will be overestimated if significant amounts of ^{36}Ar produced by the reaction $^{35}Cl(n,\gamma)^{36}Cl \rightarrow {}^{36}Ar$ are present. We, however, do not find T_{21}/T_{38} ratio >1.2 for only or mostly EH chondrites. Several EL chondrites reveal considerably lower ^{38}Ar ages, too.

According to the work of Jentsch and Schultz (1996; see also Weigel *et al.*, 1999), the possible influence of the relatively high iron content of E chondrites on the production of cosmogenic ^{21}Ne should also be considered (so-called matrix effect). Little ^{21}Ne is produced by spallation in metallic Fe itself but the flux of secondary particles and, thus, the generation of cosmogenic ^{21}Ne from Mg is significantly increased. The

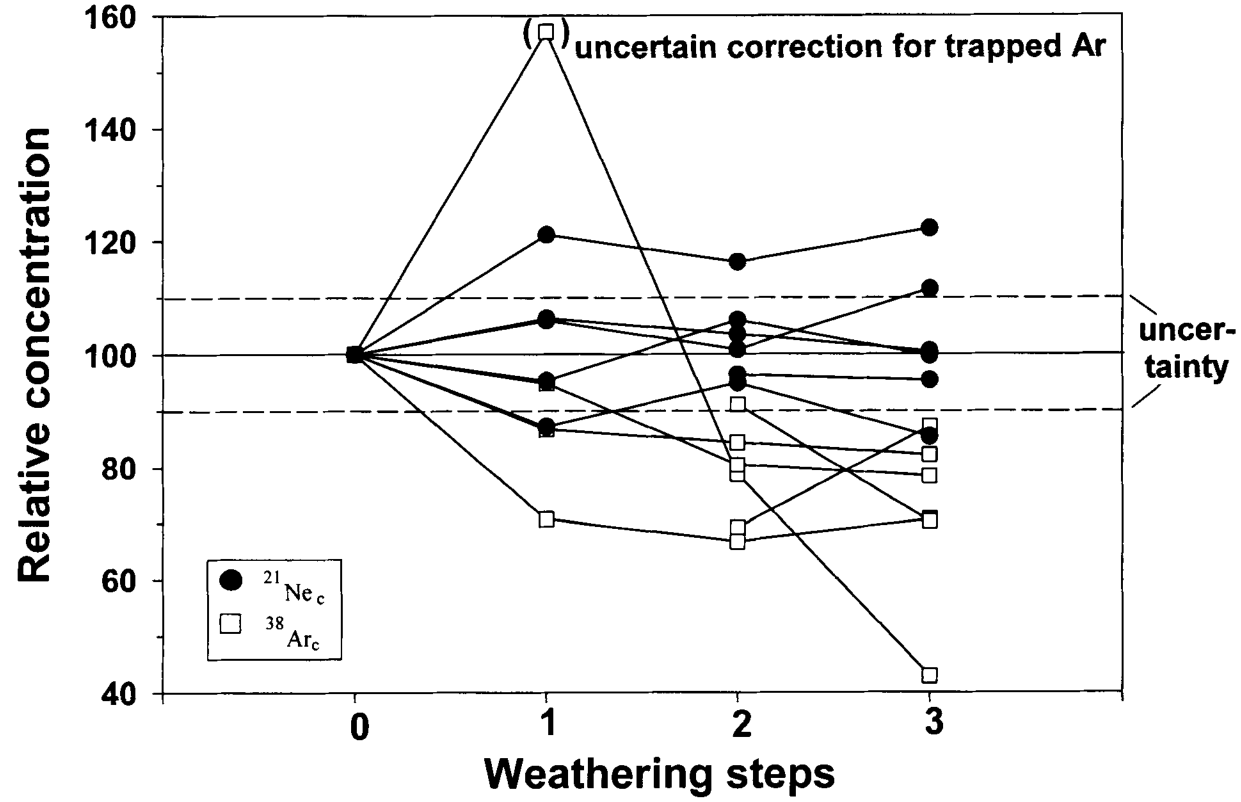

FIG. 7. Relative concentration of cosmogenic nuclides as a function of terrestrial weathering as deduced from a simple alteration experiment on E-chondritic samples. After each weathering step (four weeks intervals, see text) the noble gas content was analysed. This diagram reveals a significant change of cosmogenic ^{38}Ar in E-chondritic falls whereas cosmogenic ^{21}Ne remains relatively constant.

resulting "excess" of ^{21}Ne affects the empirical production rate model that is based on the correlation of cosmogenic $^{3}He/^{21}Ne$ and $^{22}Ne/^{21}Ne$ ratios. However, since the main target element of cosmogenic ^{21}Ne (Mg) is less abundant in E chondrites as compared to L chondrites, we expect a compensation of the matrix effect within the adopted uncertainty.

The Influence of Weathering on T_{38} of E Chondrites: A Simple Experiment

Several authors have already investigated the influence of terrestrial weathering on the noble gas content of meteorites. Decreasing abundances of radiogenic and cosmogenic noble gases have been reported for three samples of the L6-chondrite Holbrook showing different terrestrial ages (Gibson and Bogard, 1978). Another study focuses on the absorption of atmospheric rare gases and consequent alteration of the noble gas inventory of chondrites from hot deserts (Scherer *et al.*, 1994). Especially heavily weathered meteorites reveal a deficit of cosmogenic He and Ne. Most notably, however, is the absorption of atmospheric Kr and Xe. Bland *et al.* (1998) discuss the interrelation of climate and weathering. It is suggested that the degree of alteration and the formation of secondary minerals in ordinary chondrites reflect ancient climatic conditions in a given area (*i.e.*, yield a climatic signature of the time the meteorite fell). The authors reconstruct the individual stages of weathering and differentiate between an initial, rather short alteration period followed by a second stage with less erosive processes due to significant reduction of porosity and permeability.

In order to test the influence of terrestrial weathering processes on E-chondritic cosmic-ray exposure ages, we performed a simple experiment simulating some physical parameters of a semiarid region on Earth. Several E chondrites were daily wetted with rainwater and heated to 60 °C for up to 12 weeks. Additionally, the samples were alternately heated and frozen at –23 °C during the last four weeks intending to increase their porosity. For the experiment, we selected 11 falls and finds with concordant T_{21} and T_{38} (Table 1). Three individual specimens (20–80 mg) of each meteorite were measured at different stages of the simulated weathering (four weeks each). The full set of data is given by Patzer (2000).

After the treatment, the cosmogenic concentrations of ^{3}He and ^{21}Ne do not show any significant change. Taking a closer look at the amounts of cosmogenic ^{38}Ar ($^{38}Ar_c$), however, an important difference becomes obvious: While the concentrations in E-chondritic finds vary non-systematically, the abundances of $^{38}Ar_c$ in falls are generally lower than before the alteration. $^{38}Ar_c$ decreased mostly after the first weathering step (Fig. 7). This kind of loss pattern—although the time

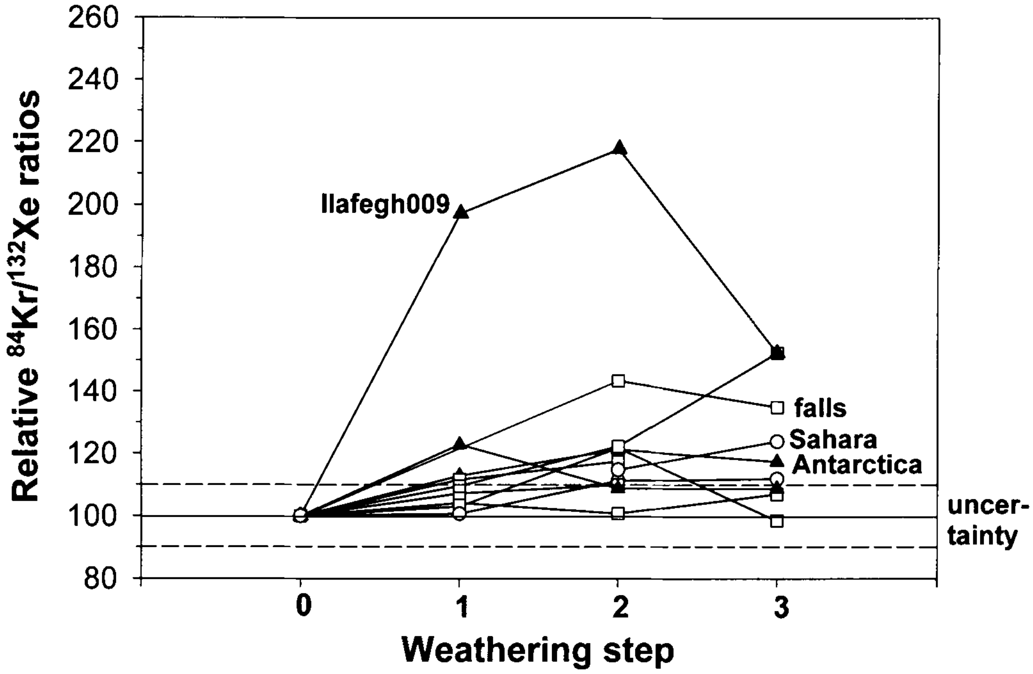

FIG. 8. In the course of the weathering experiment, concentrations of trapped atmospheric ^{132}Xe and especially ^{84}Kr increased gradually.

interval was definitely shorter than in a real situation —seems to correlate with the initial rapid weathering described by Bland *et al.* (1998). It also explains the comparatively short ^{38}Ar ages in some E chondrites that generally exhibit low trapped Ar concentrations.

We also observed the $^{84}Kr/^{132}Xe$ ratios to tend to increase with progressing alteration (Fig. 8). This kind of modification of the noble gas record can be certainly attributed to atmospheric contamination (Scherer *et al.*, 1994).

Gas Retention Ages

Gas retention ages are determined from the concentrations of U, Th, and K and their radiogenic decay products ^4He (^4He_r) and ^{40}Ar ($^{40}Ar_r$) (*e.g.*, Faure, 1986). Ideally, the gas retention ages correspond to the crystallization time of meteoritic matter. In most cases, however, continuous or sporadic thermal events possibly initiated by impact events on the parent body led to a loss of radiogenic gases. As a consequence, the calculated retention ages are lower than the actual crystallization ages and reflect the thermal history of the material. Since ^4He is already mobilized at a few hundred degrees Celsius, the corresponding U,Th-^4He_r age is more easily modified or reset than the K-$^{40}Ar_r$ age of the same sample (Anders, 1964; Wänke, 1966).

For all E chondrite samples, average K, U, and Th contents have been assumed (Mason, 1979). Most K-$^{40}Ar_r$ ages scatter around 4 Ga while U,Th-^4He_r data vary between 0.8 and 4.3 Ga (see also Crabb and Anders, 1981). Even though substantial uncertainties may apply, the ^4He_r ages apparently reflect thermal overprinting. The general trend reveals the specific diffusive behavior described for ^4He_r and $^{40}Ar_r$ above and suggests heating to at least moderate temperatures for all samples (Fig. 9, see also Table 2).

In comparison to ordinary chondrites, L chondrites show a similar age distribution except for a cluster at ~1 Ga that does not exist for E chondrites (see Schultz, 1993; see also Lipschutz and Schultz, 1999). H chondrites, on the other hand, exhibit a very different age pattern with a distinct cluster at around 4 to 4.5 Ga. Obviously, each meteorite class is characterized by individual age clusters caused by different metamorphic events on their parent bodies.

CONCLUSIONS

Cosmic ray exposure ages of E chondrites mainly range between 2 and 50 Ma and show a similar spectrum to ordinary chondrites. Three clusters at about 3.5, 8 and 25 Ma are slightly visible indicating possible catastrophic impact events on the E-chondrite parent body(ies). No systematic trends are apparent among the cosmic-ray exposure ages of either the subgroups or the petrologic types. The majority of EL6 samples though exhibits exposure ages around or above 20 Ma.

Several meteorites show significant discrepancies in cosmic-ray exposure ages derived from different cosmogenic noble gas nuclides. Higher $^{38}Ar_c$ exposure ages compared to those calculated from $^{21}Ne_c$ can be at least partly explained by insufficient correction if the amount of trapped noble gases is high. In other cases, we found significantly lower $^{38}Ar_c$ age values. For these E chondrites, we suggest terrestrial weathering causing depletion of cosmogenic ^{38}Ar in mineral phases that contain Ca and Fe (*i.e.*, the main target elements of

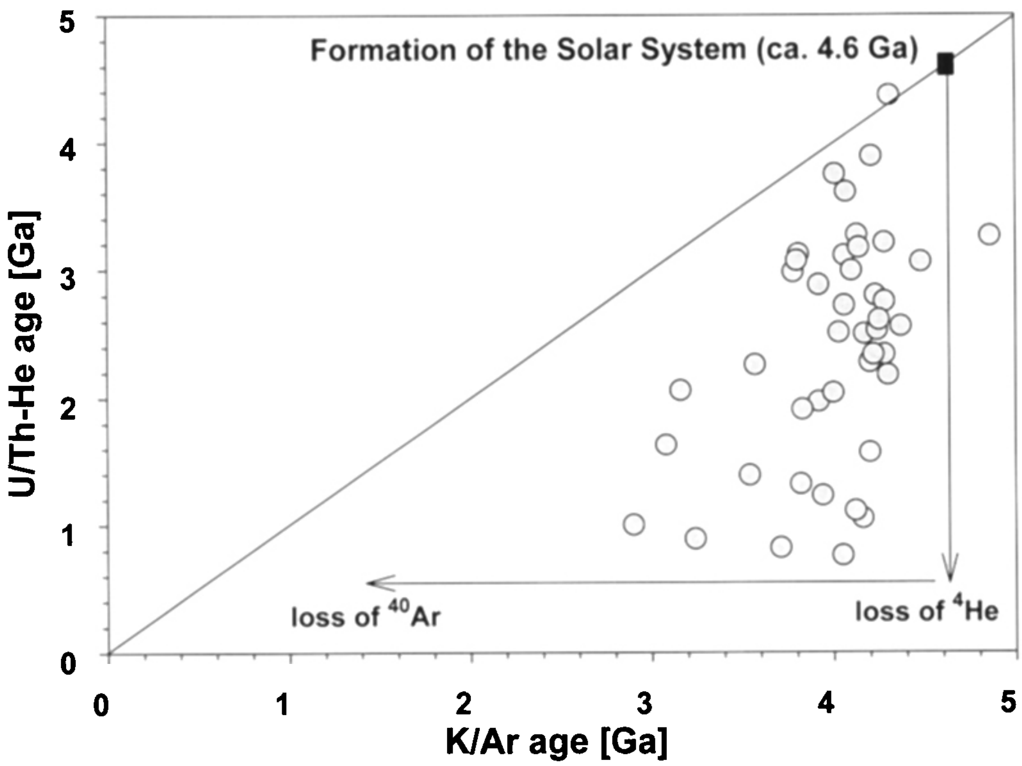

FIG. 9. U/Th-^{4}He and K-^{40}Ar gas retention ages of E chondrites. All data points show He and Ar losses indicating that metamorphic events were taking place on the parent body(ies) of these meteorites.

$^{38}Ar_c$ production). This was proven by a simple weathering experiment, which led to systematically decreased concentrations of cosmogenic ^{38}Ar. The simulated alteration also induced an increase of absorbed terrestrial atmospheric Kr and Xe.

Gas retention ages of E chondrites are generally less than 4.6 Ga and, hence, influenced by metamorphic overprinting. Most K-^{40}Ar ages scatter around 4 Ga. The U,Th-^{4}He ages vary considerably below this value reflecting higher losses of radiogenic ^{4}He. Overall, the thermal history of E chondrites seems to be different from that of ordinary chondrites.

Acknowledgements–We thank the following institutions for providing meteorite samples for this study: NASA Johnson Space Center (Houston, USA), the National Science Foundation (NSF) that supports the Antarctic Search for Meteorites (ANSMET), the National Institute of Polar Research (Tokyo, Japan), the University of Münster (Germany), the Natural History Museum (London, U.K.), and Le Musée National d'Histoire (Paris, France). We also thank Siegfried Hermann for technical assistance and Yuri A. Shukolyukov for providing the Kaidun data. Last but not least, we thank Andreas Weigel, Don Bogard, and Ed Scott (the associate editor) for their reviews and helpful comments on this paper.

Editorial handling: E. R. D. Scott

REFERENCES

ANDERS E. (1964) Origin, age, and composition of meteorites. *Space Sci. Rev.* **3**, 583–714.

BEGEMANN F., EBERHARDT P. AND HESS D. C. (1959) ^{3}He-^{3}H Strahlungsalter eines Steinmeteoriten. *Z. Naturforschg.* **14A**, 500–503.

BENOIT P. H., SEARS D. W. G., AKRIDGE J. M. C., BLAND P. A., BERRY F. J. AND PILLINGER C. T. (2000) The non-trivial problem of meteorite pairing. *Meteorit. Planet. Sci.* **35**, 393–406.

BLAND P. A., SEXTON A. S., JULL A. J. T., BEVAN A. W. R., BERRY F. J., THORNLEY D. M., ASTIN T. R., BRITT D. T. AND PILLINGER C. T. (1998) Climate and rock weathering: A study of terrestrial age dated ordinary chondritic meteorites from hot desert regions. *Geochim. Cosmochim. Acta* **62**, 3169–3184.

CRABB J. AND ANDERS E. (1981) Noble gases in E-chondrites. *Geochim. Cosmochim. Acta* **45**, 2443–2464.

CRABB J. AND ANDERS E. (1982) On the siting of noble gases in E-chondrites. *Geochim. Cosmochim. Acta* **46**, 2351–2361.

CRESSY P. J. AND BOGARD D. D. (1976) On the calculation of cosmic-ray exposure ages of stony meteorites. *Geochim. Cosmochim. Acta* **40**, 749–762.

CHRISTOPHE-MICHEL-LÉVY M. AND BOUROT-DENISE M. (1988) A new look at the Galim (a) and Galim (b) meteorites. *Mineral. Mag.* **52**, 519–525.

EASTON A. J. AND ELLIOTT C. J. (1977) Analyses of some meteorites from the British Museum (Natural History) Collection. *Meteoritics* **12**, 409–416.

EBERHARDT P., EUGSTER O., GEISS J. AND MARTI K. (1966) Rare gas measurements in 30 stone meteorites. *Z. Naturforsch.* **A21**, 414–426.

EUGSTER O. (1988) Cosmic-ray production rates for ^{3}He, ^{21}Ne, ^{38}Ar, ^{83}Kr, and ^{126}Xe in chondrites based on ^{81}Kr-Kr exposure ages. *Geochim. Cosmochim. Acta* **52**, 1649–1662.

EUGSTER O., WEIGEL A. AND POLNAU E. (1997) Ejection times of Martian meteorites. *Geochim. Cosmochim. Acta* **61**, 2749–2757.

FAURE G. (1986) *Principles of Isotope Geology*. 2nd ed., John Wiley & Sons, New York, New York, USA. 589 pp.

GIBSON E. K., JR. AND BOGARD D. D. (1978) Chemical alterations of the Holbrook chondrite resulting from terrestrial weathering. *Meteoritics* **13**, 277–289.

GLADMAN B. *ET AL.* (1997) Dynamical lifetimes of objects injected into the asteroid belt resonances. *Science* **277**, 197–201.

GRAF T. AND MARTI K. (1989) Exposure ages of H-chondrites and parent body structure (abstract). *Lunar Planet. Sci.* **20**, 353–354.

GRAF T. AND MARTI K. (1991) Exposure ages of LL- and L/LL-chondrites and implications for parent body history (abstract). *Meteoritics* **26**, 340.

GRAF T. AND MARTI K. (1992) Cosmic-ray exposure ages of enstatite meteorites (abstract). *Meteoritics* **27**, 227.

GROSSMAN J. N. (2000) The Meteoritical Bulletin, No. 84, 2000 August. *Meteorit. Planet. Sci.* **35 (Suppl.)**, A199–A225.

HERTOGEN J., JANSSENS M. J., TAKAHASHI H., MORGAN J. W. AND ANDERS E. (1983) Enstatite chondrites: Trace element clues to their origin. *Geochim. Cosmochim. Acta* **47**, 2241–2255.

HERZOG G. F., VOGT S., ALBRECHT A., XUE S., FINK D., KLEIN J., MIDDLETON R., WEBER H. AND SCHULTZ L. (1997) Complex exposure histories for meteorites with "short" exposure ages. *Meteorit. Planet. Sci.* **32**, 413–422.

HINTENBERGER H., SCHULTZ L. AND WÄNKE H. (1966) Messung der Diffusionsverluste von radiogenen und spallogenen Edelgasen in Steinmetetoriten II. *Z. Naturforsch.* **19A**, 1147–1159.

IVANOV A. V., ULYANOV A. A., SKRIPNIC A. Y. AND KONOKOVA N. N. (1984) The Kaidun polymict carbonaceous breccia: A mixture of incompatible types of meteorites (abstract). *Lunar Planet. Sci.* **15**, 393–394.

JAROSEWICH E. (1990) Chemical analyses of meteorites: A compilation of stony and meteorite analyses. *Meteoritics* **25**, 323–337.

JENTSCH O. AND SCHULTZ L. (1996) Cosmogenic noble gases in silicate inclusions of iron meteorite: Effects of bulk composition on elemental production rates. *J. Roy. Soc. West. Australia* **79**, 67–71.

KALLEMEYN G. W. AND WASSON J. T. (1986) Compositions of enstatite (EH3, EH4,5 and EL6) chondrites: Implications regarding their formation. *Geochim. Cosmochim. Acta* **50**, 2153–2164.

KEIL K. (1989) Enstatite meteorites and their parent bodies. *Meteoritics* **24**, 195–208.

KIMURA M. AND LIN Y. (1999) Petrologic and mineralogical study of enstatite chondrites with reference to their thermal histories. *Antarctic Meteorite Res.* **12**, 1–18.

KONG P., MORI T. AND EBIHARA M. (1997) Compositional continuity of enstatite chondrites and implications for heterogeneous accretion of the enstatite chondrite parent body. *Geochim. Cosmochim. Acta* **61**, 4895–4914.

LEYA I., LANGE H-J., NEUMANN S., WIELER R. AND MICHEL R. (2000) The production of cosmogenic nuclides in stony meteoroids by galactic cosmic ray particles. *Meteorit. Planet. Sci.* **35**, 259–286.

LIN Y. AND KIMURA M. (1997) Thermal histories and parent body(ies) of EH chondrites: Evidence from new highly equilibrated EHs (Y793225, 82189, 8404, 8414 and 86004) (abstract). *Lunar Planet. Sci.* **28**, 817–818.

LIPSCHUTZ M. E. AND SCHULTZ L. (1999) Meteorites. In *Encyclopedia of the Solar System* (eds. P. R. Weissman, L-A. McFadden and T. V. Johnson), pp. 629–671. Academic Press, San Diego, California, USA.

LOEKEN TH., SCHERER P., WEBER H. W. AND SCHULTZ L. (1992) Noble gases in eighteen stone meteorites. *Chem. Erde* **52**, 249–259.

LORIN J. C. AND PELLAS P. (1979) Preirradiation history of Djermaia (H) chondrite breccia. *Icarus* **40**, 502–509.

MARTI K. AND GRAF T. (1992) Cosmic-ray exposure history of ordinary chondrites. *Ann. Rev. Earth Planet. Sci.* **20**, 221–243.

MASON B. (1966) The enstatite chondrites. *Geochim. Cosmochim. Acta* **30**, 23–39.

MASON B. (1979) Cosmochemistry, Meteorites. In *Data of Geochemistry* (ed. F. Fleischer), pp. B1–B132. Geological Survey Professional Paper 440-B-1, Washington, D.C., USA.

MASON B. (1992) Petrographic descriptions. *Antarctic Meteorite Newsletter* **15**, 17.

METBASE (1999) Version 4.0 for Windows–Meteorite Data Retrieval Software © Jörn Koblitz, Fischerhude, Germany.

MICHEL R. *ET AL.* (1997) Cross sections for the production of residual nuclides by low- and medium-energy protons from the target elements C, N, O, Mg, Al, Si, Ca, Ti, V, Mn, Fe, Co, Ni, Cu, Sr, Y, Zr, Nb, Ba and Au. *Nucl. Instrum. Methods Phys. Res.* **B129**, 153.

MORBIDELLI A. AND GLADMAN B. J. (1998) Orbital and temporal distributions of meteorites originating in the asteroid belt. *Meteorit. Planet. Sci.* **33**, 999–1016.

NISHIIZUMI K., REGNIER S. AND MARTI K. (1979) Cosmic ray exposure ages of meteorites: A recalibration. *Meteoritics* **14**, 499–500.

NISHIIZUMI K., REGNIER S. AND MARTI K. (1980) Cosmic ray exposure ages of chondrites, pre-irradiation and constancy of cosmic ray flux in the past. *Earth Planet. Sci. Lett.* **50**, 156–170.

OKAZAKI R., TAKAOKA N., NAKAMURA T. AND NAGAO K. (1998) Cosmogenic noble gases in E-chondrites. *Symp. Antarct. Meteor.* **23**, 120–122.

OZIMA M. AND PODOSEK F. A. (1983) *Noble Gas Geochemistry*. Cambridge Univ. Press, Cambridge, U.K. 367 pp.

PATZER A. (2000) Edelgase in Enstatit-Chondriten. Ph.D. thesis, Johannes-Gutenberg-Universitaet Mainz, Mainz, Germany. 120 pp.

PATZER A. AND SCHULTZ L. (1999) Do weathering effects influence cosmic ray exposure ages of enstatite chondrites? In *Workshop on Extraterrestrial Materials from Cold and Hot Deserts* (ed. L. Schultz *et al.*), pp. 67–68. LPI Contribution **997**, Lunar and Planetary Institute, Houston, Texas, USA.

PATZER A., SCHERER P., WEBER H. W. AND SCHULTZ L. (1999) New exposure ages of chondrites: Short transfer times from asteroid belt to Earth? (abstract). *Lunar Planet. Sci.* **30**, #1145, Lunar and Planetary Institute, Houston, Texas, USA (CD-ROM).

REEDY R. C. (1985) A model for GCR-particle fluxes in stony meteorites and production rates of cosmogenic nuclides. *Proc. Lunar Planet. Sci. Conf.* **15th**, *J. Geophys. Res.* **90**, C722–C728.

RUBIN A. E. (1997) Mineralogy of meteorite groups. *Meteorit. Planet. Sci.* **32**, 231–247.

RUBIN A. E. AND SCOTT E. R. D. (1997) Abee and related EH chondrite impact-melt breccias. *Geochim. Cosmochim. Acta* **61**, 425–435.

RUBIN A. E., SCOTT E. R. D. AND KEIL K. (1997) Shock metamorphism of enstatite chondrites (abstract). *Lunar Planet. Sci.* **26**, 1197–1198.

SCHERER P., SCHULTZ L. AND LOEKEN T. (1994) Weathering and Atmospheric Noble Gases in Chondrites. In *Noble Gas Geochemistry and Cosmochemistry* (ed. J. Matsuda), pp. 43–53. Terra Science Publishing Company, Tokyo, Japan.

SCHERER P., HERRMANN S. AND SCHULTZ L. (1998) Noble gases in twenty-one Saharan LL-chondrites: Exposure ages and possible pairings. *Meteorit. Planet. Sci.* **33**, 259–265.

SCHULTZ L. (1993) *Planetologie–Eine Einführung*. Birkhäuser Verlag, Berlin, Germany. 270 pp.

SCHULTZ L. AND FRANKE L. (2000) *Helium, Neon, and Argon in Meteorites–A Data Compilation*. Max-Planck-Institut für Chemie, Mainz, Germany (CD-ROM).

SCHULTZ L. AND FREUNDEL M. (1985) On the production rate of ^{21}Ne in ordinary chondrites. In *Isotopic Ratios in the Solar System* (ed. Centre National d'Etudes Spatiales), pp. 27–33. Cepadues-Editions, Toulouse, France.

SCHULTZ L. AND SIGNER P. (1977) Noble gases in the St. Mesmin chondrite: Implications to the irradiation history of a brecciated meteorite. *Earth Planet. Sci. Lett.* **36**, 363–371.

SCHULTZ L. AND WEBER H. (1995) Exposure ages of H chondrites with helium loss. *Meteoritics* **30**, 575–576.

SCHULTZ L. AND WEBER H. (1997) Exposure age distribution of H-chondrites with and without helium loss (abstract). In *Isotopes in the Solar System* (eds. J. N. Goswami, S. Sahijpal and P. Chakrabarty), pp. 34–35. Physical Research Lab., Ahmedabad, India.

SCHULTZ L., SIGNER P., LORIN J. C. AND PELLAS P. (1972) Complex irradiation history of the Weston chondrite. *Earth Planet. Sci. Lett.* **15**, 403–410.

SCHULTZ L., WEBER H. W. AND BEGEMANN F. (1991) Noble gases in H-chondrites and potential differences between Antarctic and non-Antarctic meteorites. *Geochim. Cosmochim. Acta* **55**, 59–66.

SEARS D. W. G. (1980) Formation of E-chondrites and aubrites—A thermodynamic model. *Icarus* **43**, 184–202.

SEARS D. W. G., KALLEMEYN G. W. AND WASSON J. T. (1982) The compositional classification of chondrites–II. The enstatite chondrite groups. *Geochim. Cosmochim. Acta* **46**, 597–608.

VAN SCHMUS W. R. AND WOOD J. A. (1967) A chemical–mineralogical classification for the chondrite meteorites. *Geochim. Cosmochim. Acta* **31**, 747–765.

WACKER J. F. AND MARTI K. (1983) Noble gas components in clasts and separates of the Abee meteorite. *Earth Planet. Sci. Lett.* **62**,147–158.

WÄNKE H. (1966) Meteoritenalter und verwandte Probleme der Kosmochemie. *Fortschr. Chem. Forsch.* **7**, 322–408.

WEEKS K. S. AND SEARS D. W. G. (1985) Chemical and physical studies of type 3 chondrites–V: The enstatite chondrites. *Geochim. Cosmochim. Acta* **49**, 1525–1536.

WEIGEL A., EUGSTER O., KOEBERL C., MICHEL R., KRAEHENBUEHL U. AND NEUMANN S. (1999) Relationships among lodranites and acapulcoites: Noble gas isotopic abundances, chemical composition, cosmic-ray exposure ages, and solar cosmic ray effects. *Geochim. Cosmochim. Acta* **63**, 175–192.

ZAEHRINGER J. AND GENTNER W. (1960) Zum Xe^{129} in dem Meteoriten Abee. *Z. Naturforschg.* **16a**, 239–242.

ZHANG Y., BENOIT P. H. AND SEARS D. W. G. (1995) The classification and complex thermal history of the enstatite chondrites. *J. Geophys. Res.* **100**, 9417–9438.